DOI: 10.1002/cssc.201200866

Electrooxidation of Ethylene Glycol and Glycerol on Pd-(Ni-Zn)/C Anodes in Direct Alcohol Fuel Cells

Andrea Marchionni,[a] Manuela Bevilacqua,[a] Claudio Bianchini,[a] Yan-Xin Chen,[a, b] Jonathan Filippi,[a] Paolo Fornasiero,[b] Alessandro Lavacchi,[a] Hamish Miller,[a] Lianqin Wang,[a, b] and Francesco Vizza*[a]

The electrooxidation of ethylene glycol (EG) and glycerol (G) has been studied: in alkaline media, in passive as well as active direct ethylene glycol fuel cells (DEGFCs), and in direct glycerol fuel cells (DGFCs) containing Pd-(Ni-Zn)/C as an anode electrocatalyst, that is, Pd nanoparticles supported on a Ni–Zn phase. For comparison, an anode electrocatalyst containing Pd nanoparticles (Pd/C) has been also investigated. The oxidation of EG and G has primarily been investigated in half cells. The results obtained have highlighted the excellent electrocatalytic activity of Pd-(Ni-Zn)/C in terms of peak current density, which is as high as 3300 $A g_{(Pd)}^{-1}$ for EG and 2150 $A g_{(Pd)}^{-1}$ for G. Membrane-electrode assemblies (MEA) have been fabricated using Pd-(Ni-Zn)/C anodes, proprietary Fe-Co/C cathodes, and Tokuyama A-201 anion-exchange membranes. The MEA performance has been evaluated in either passive or active cells fed with aqueous solutions of 5 wt% EG and 5 wt% G. In view of the peak-power densities obtained in the temperature range from 20 to 80 °C, at Pd loadings as low as 1 mg cm^{-2} at the anode, these results show that Pd-(Ni-Zn)/C can be classified amongst the best performing electrocatalysts ever reported for EG and G oxidation.

Introduction

The selective conversion/production of chemicals from renewable resources with simultaneous production of energy is perhaps one of the most desirable targets in sustainable chemistry.[1] The realization of such processes will provide energy with no overall CO_2 emissions and at the same time lead to the production of industrially relevant feedstocks. Indeed, starting from renewable alcohols, a large variety of products such as aldehydes, ketones, and carboxylic acids might be obtained. Recent results have shown that direct fuel cells can be effectively employed to convert alcohols into various oxygenates, providing at the same time good power densities, exploiting the ability of certain anode electrocatalysts to bring about the partial oxidation of the anolyte with high selectivity and fast kinetics.

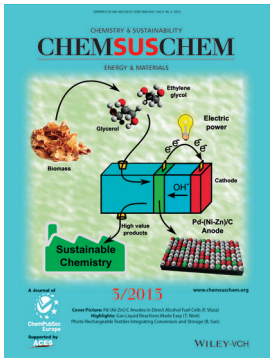

COVER

The selective conversion of ethanol into acetic acid has been demonstrated in direct ethanol fuel cells (DEFCs) equipped with anion-exchange membranes. In the most successful cases, Pd metal was the major component of the anode electrocatalyst. Alcohols with a higher molecular weight than ethanol are now arousing great interest as fuels in direct alcohol fuel cells (DAFC) for various reasons, among which the relatively low toxicity, high boiling point, high specific energy, and the capacity of some of them to be renewable. Included in this group are ethylene glycol (EG) and glycerol (G).

EG has a volumetric energy density of 5.9 KWh L^{-1} and can be produced by heterogeneous hydrogenation of cellulose derivatives.[2,3] G has a volumetric energy density of 6.3 KWh L^{-1} and is the by-product of biodiesel production. As such, it is inexpensive (0.3 US$ kg^{-1}) and largely available (2.4 million tonnes per year). Moreover, the increasing demand for methyl esters as fuel additives is expected to increase the G production, thus leading to further cost reduction.[4] It is also important to stress that some EG and G oxidation products, such as glycolic acid, oxalic acid, glyceric acid, tartronic acid, mesoxalic acid, and 1,3 dihydro-acetone, are valuable fine chemicals, currently produced by costly and non-environmentally friendly processes. Indeed, G oxidation reactions are generally performed with stoichiometric oxidants, such as permanganate, nitric acid or chromic acid, and are characterized by low yields and selectivity.[5] Fermentation processes exhibit higher oxidation selectivity, but have a low conversion rate. Alternatively, one may apply heterogeneous catalytic processes with molec-

[a] Dr. A. Marchionni, Dr. M. Bevilacqua, Dr. C. Bianchini, Dr. Y.-X. Chen, Dr. J. Filippi, Dr. A. Lavacchi, Dr. H. Miller, Dr. L. Wang, Dr. F. Vizza
Istituto di Chimica dei Composti Organometallici
Consiglio Nazionale delle Ricerche
via Madonna del Piano 10, 50019 Sesto Fiorentino (Italy)
Fax: (+39) 0555225203
E-mail: francesco.vizza@iccom.cnr.it

[b] Dr. Y.-X. Chen, Dr. P. Fornasiero, Dr. L. Wang
Department of Chemistry
ICCOM-CNR-Trieste
CENMAT, University of Trieste
via L. Giorgeri 1, 34127 Trieste (Italy)

ular oxygen as oxidant, but these processes are generally characterized by harsh conditions and low selectivity, and as a consequence low sustainability.[6–10]

The conversion of G or EG into oxygenated compounds in DAFCs has been achieved on Pt-based anodes, yet none of these catalysts has demonstrated the capacity to produce both high power densities and high product selectivities. Recently, Li and co-workers[11,12] have reported a maximum power density of 71 mW cm^{-2} at 50 °C in a direct ethylene glycol fuel cell (DEGFC) and a maximum power density of 124.5 mW cm^{-2} at 80 °C in a direct glycerol fuel cell (DGFC), both equipped with an anion-exchange membrane, Pt/C anode, and Fe-Cu/C cathode. In their elegant articles, these authors have provided evidence for a good selectivity towards higher-value chemicals by tuning the fuel cell operation voltage. Martemianow et al.[13] have improved the electrode membrane assembly (MEA) fabrication (Pt and Pt-based bimetallic anode) in a DGFC and selected appropriate experimental conditions (i.e., fuel composition, fuel flow) to optimize the cell performance, so as to obtain a power density of 24 mW cm^{-2} at 80 °C. Atanassov et al.[14] have investigated the electrooxidation of EG and G on Pt-based binary and ternary nanostructured catalysts synthesized by spray pyrolysis. These authors were able to demonstrate that the addition of Ru and Sn to Pt has a beneficial effect on the oxidation of EG and G. Koper et al.[15] have obtained a very high selectivity in the oxidation of G to dihydroxyacetone in acidic media on a Pt/C catalyst in the presence of Bi dissolved in the electrolytic solution.

Palladium-based electrocatalysts are the best materials for the oxidation of G and EG. Shen and Xu were the first authors to demonstrate that Pd adsorbed onto oxide/C materials yield electrocatalysts for alcohol oxidation with a much higher catalytic activity (i.e., onset oxidation potential and peak current density) and electrochemical stability with respect to any other known Pd/C or Pt/C catalyst under comparable experimental conditions (C = Vulcan).[16–18] Out of all the electrocatalysts investigated, Pd-Co_3O_4 showed the highest activity for the electrooxidation of EG and G.[19] The synergistic effect of palladium alloyed to platinum has been observed by Coutanceau et al. for the oxidation of EG in alkaline media in both, half-cell and DAFC tests.[20,21] These authors have also studied the capacity of Pd to depress C–C bond cleavage and enhance the catalyst lifetime, by investigating the EG oxidation on PtPd, PtPdBi, and PtBi catalysts. On these electrocatalysts, EG is converted into mixtures of glycolic acid, glyoxylic acid, oxalic acid, and formic acid, but the relative composition depends upon the anode catalyst employed. It has been proposed that Bi favors the adsorption of OH^- species and also affects the product distribution by depressing C–C bond cleavage. A mechanism of EG oxidation has been proposed by Coutanceau.[22]

We have recently reported that the electrooxidation of EG on Pd/C, Pd (Ni-Zn)/C anodes, and on a smooth Pd electrode is dramatically influenced by the pH value of the anolyte as well as the catalyst structure.[23] Recently, we also published data on the activity of palladium nanoparticles supported on multiwalled carbon nanotubes (Pd/MWNCT) towards the electrooxidation of alcohols. The performance of Pd/MWNCT was evaluated in a DGFC that gave rise to a peak power density of 7 mW cm^{-2} at room temperature and 80 mW cm^{-2} at 80 °C.[24]

To the best of our knowledge, all known Pd- or Pt-based electrocatalysts cannot promote the complete oxidation of EG or G to CO_2 in alkaline media. EG or G may undergo C–C bond scission with formation of CO_2, yet this is invariably a minor reaction pathway compared to the oxidation to carboxylates which, in turn, is not completely selective. There is little doubt that the nature, structure, and composition of the anode electrocatalyst have a crucial effect on the oxidation in terms of power output, Faradaic efficiency, and product selectivity. In this respect, much research work is still needed to design and develop improved catalysts for polyalcohol oxidation in DAFCs.

Herein, we describe the cogeneration of electrical energy and higher-value chemicals from the electrooxidation of EG and G in both passive and active alkaline DAFCs in which Ni foam anodes are coated with a Pd-(Ni-Zn)/C catalyst and the cathodes are noble metal free, containing exclusively a Fe–Co/C (C = Ketjen Black) catalyst. For comparative purposes, we have also investigated the EG and G electrooxidation on a nanostructured Pd/C catalyst prepared by chemical reduction of H_2PdCl_4 adsorbed on C.[25]

Results and Discussion

Electrochemical oxidation of ethylene glycol and glycerol on Pd(Ni-Zn)/C and Pd/C in half cells

In a previous publication, we described the synthesis of a catalytic material obtained by a redox trans-metalation process involving the spontaneous deposition of palladium onto Ni–Zn alloys supported on Vulcan XC-72. The characterization of the resulting Pd-(Ni-Zn)/C material using high-resolution TEM (HRTEM; see Figure 1), extended X-ray absorption fine structure (EXAFS), powder X-ray powder diffraction (XPRD), and X-ray absorption near edge structure (XANES) techniques has shown that its surface contains small (0.5–1 nm from EXAFS estimation and average diameter of 2.3 nm from HRTEM, as reported in Figure 1), highly dispersed aggregates of Pd and Ni clusters as well as single Pd sites, probably stabilized by the interaction with oxygen atoms from Ni–O moieties.[25] As a reference material, nanostructured Pd/C was also synthesized by the reduction of an aqueous solution of $PdCl_2$/HCl with ethylene glycol in the presence of Vulcan XC-72. In Pd/C the particles are larger, less dispersed, and much less crystalline than Pd-(Ni-Zn)/C. In the work presented here we investigated the electrochemical performance of these catalysts in the electrooxidation of EG and G in half-cells as well as in passive and active polymer electrolyte membrane fuel cells, with the aim to achieve cogeneration of electricity and valuable chemicals.

The electrochemical activity of the nano-structured catalysts Pd-(Ni-Zn)/C and Pd/C for EG and G oxidation was first investigated by cyclic voltammetry (CV) at room temperature in deoxygenated 2 M KOH solutions. A series of cyclic voltammograms recorded at KOH concentrations ranging from 0.5 to 4 M show the generation of the highest current density in the

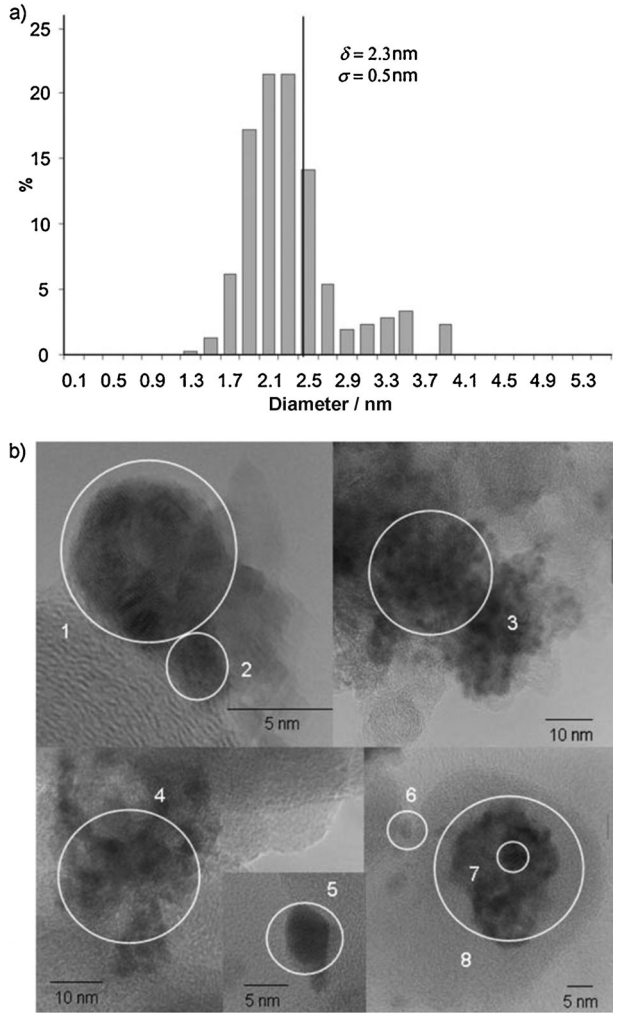

Figure 1. a) HRTEM histograms of particle volume distribution versus diameter for Pd-(Ni-Zn)/C. The average size (δ) and standard deviation (σ) are reported. b) HRTEM images of Pd-(Ni-Zn)/C at different magnifications; spots of energy-dispersive X-ray (EDX) analysis are shown in circles; Pd/Ni relative compositions as detected by EDX integrated peak areas: 1) Ni > Pd with Ni (110) plane fringes; 2) Ni(111) plane fringes; 3) Pd/Ni = 1:2; 4) Pd/Ni = 1:1; 5) Pd with cuboctahedron crystal facets; 6) Ni; 7) Pd (110) plane fringes; 8) Pd > Ni; minor O contribution are also present in all cases. From Ref. [25].

range of 1–1.5 M KOH. However, all the following electrochemical studies, either in half-cell or in monoplanar cell (passive or active), were performed using a 2 M KOH solution to keep the concentration of the OH^- group as constant as possible in all experiments. The oxidation of EG and G in alkaline media consumes OH^- groups, irrespective of the oxidation level of the substrate.[27] All the CV measurements were performed at a sweep rate of 50 mV s^{-1} in solutions containing 5 wt% EG or 5 wt% G using glassy carbon electrodes with a Pd loading between 24 and 30 μg cm^{-2}, corresponding to 3.5–4.0 mg of catalyst ink. Relevant electrochemical parameters such as peak current density (J_p), specific peak current density (Sa_p), and forward anodic peak potential (E_p), are listed in Table 1 for the fuels investigated.

The cyclic voltammograms of EG oxidation on Pd/C and Pd-(Ni-Zn)/C electrodes are shown in Figure 2.[23] The two electrocatalysts both show high activity towards the oxidation of EG with an onset potential at approximately 0.4 V (versus RHE) and high specific current densities of 3.33 mA $\mu g_{(Pd)}^{-1}$ for Pd-(Ni-Zn)/C and of 2.76 mA $\mu g_{(Pd)}^{-1}$ for Pd/C. As shown by the trace in Figure 2, the electrocatalyst Pd-(Ni-Zn)/C is more active than Pd/C especially in terms of forward anodic peak potential with the intensity controlled by the progressive coverage of the two electrodes surfaces by PdO at high potentials.[25] The reverse scans show two further anodic peaks owing to the oxidation of fresh EG on the catalysts freed from PdO.[28] Accordingly, Pd-(Ni-Zn)/C and Pd/C can be considered amongst the best performing electrocatalysts ever reported for EG oxidation. Figure 3 shows the cyclic voltammograms of the G oxidation reaction on Pd/C and Pd-(Ni-Zn)/C electrodes. As expected, the oxidation of G starts at the potential corresponding to the coverage of the electrode surface by OH groups.[23–25,29,30] As shown by the traces in Figure 3, the two electrocatalysts are characterized by rather similar activities, especially in terms of forward and backward anodic peak potentials, with onset potentials of around 0.41 V (versus RHE) and specific current densities higher than 2.0 mA $\mu g_{(Pd)}^{-1}$ (see Table 1), which, though they are lower than those obtained for EG, are remarkable results indeed. We are not aware of such a performance in G oxidation in half cell experiments with any known electrocatalyst (Table 2) especially at the very low metal loadings used in this work. The only exception is a Pd/MWNCT anode catalyst,[24] even if the data reported in Table 2 are not exactly com-

Table 1. CV data for the electrooxidation of 5 wt% EG and G in 2 M KOH on Pd-(Ni-Zn)/C and Pd/C.

Fuel	Catalyst	J_p [mA cm^{-2}]	Sa_p [mA μg_{Pd}^{-1}]	E_{onset} [V]	E_p [V]
EG	Pd/C	64.0	2.76	0.42	0.83
	Pd-(Ni-Zn)/C	84.2	3.33	0.39	0.90
G	Pd/C	55.5	2.10	0.41	0.95
	Pd-(Ni-Zn)/C	65.3	2.15	0.42	0.92

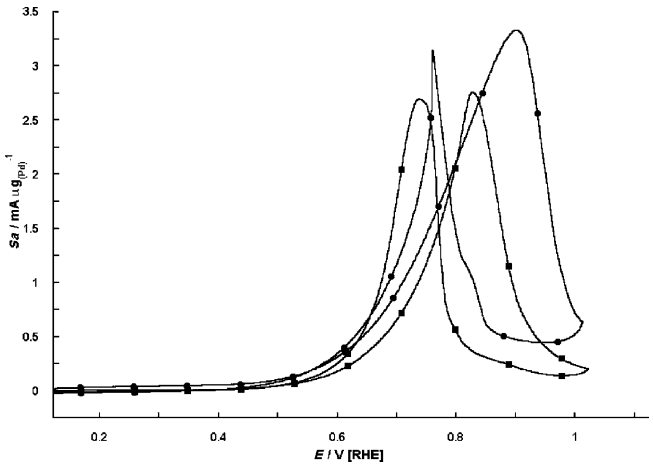

Figure 2. Cyclic voltammograms (tenth cycle) of EG oxidation on Pd-(Ni-Zn)/C (●) and Pd/C (■)electrodes in 2 M KOH and 5 wt% EG. Scan rate: 50 mV s^{-1}.

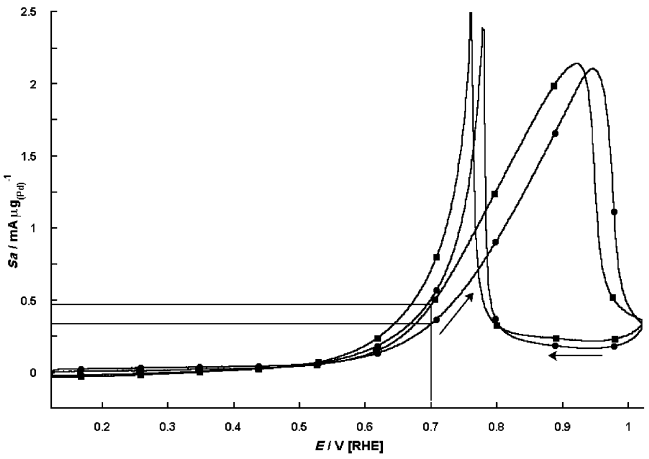

Figure 3. Cyclic voltammograms (tenth cycle) of G oxidation on Pd-(Ni-Zn)/C (■) and Pd/C (●) electrodes in 2 M KOH and 5 wt% G. Scan rate: 50 mV s^{-1}.

Table 2. CV data for Pt and Pd-based anode catalysts for G electrooxidation.

Catalyst	Anolyte	Load [μg cm^{-2}]	*J* [mA cm^{-2}] peak	@0.5 V	*Sa* [mA $μg_{(Pd)}^{-1}$] peak	@0.5 V	Ref.
Pd-(NiZn)-C	5 wt% G; 2 M KOH	25	53.5	1.0	2.140	0.040	this work
Pd/C	5 wt% G; 2 M KOH	31.1	65.3	1.6	2.100	0.050	this work
Pd-NiO/C	1 M G; 1 M KOH	300	88.1	0.0	0.294	0	[16]
Pt/C 40%	1 M G; 1 M KOH	81.5	32.5	1.3	0.399	0.016	[12]
Pd/C 36%	0.1 M G; 1 M KOH	141.5	24.6	0	0.174	0	[22]
Pt/C 37%	0.1 M G; 1 M KOH	141.5	24.3	1.48	0.172	0.010	[22]
$Pd_{0.9}Bi_{0.1}$/C 38%	0.1 M G; 1 M KOH	141.5	31.2	1.17	0.220	0.008	[22]
$Pt_{0.9}Bi_{0.1}$/C 36%	0.1 M G; 1 M KOH	141.5	31.4	12.2	0.222	0.086	[22]
$Pt_{0.45}Pd_{0.45}Bi_{0.1}$/C 38%	0.1 M G; 1 M KOH	141.5	38.5	12.4	0.272	0.088	[22]
Pd/CPAA 50%	1 M G; 1 M KOH	300	71.9	1.85	0.240	0.006	[31]
Pd/MWCNT	5% G; 2 M KOH	17.0	47.6	2.16	2.8	0.127	[24]

parable because the experiments were not performed with the same metal loading. Also in this case, as for the oxidation of EG, the backward scan peak can be associated with the oxidation of freshly chemisorbed G. Previous CV studies of ethanol oxidation on Pd have shown that the decrease in current at high voltages is mainly owed to the formation of a PdO layer, which blocks the adsorption of the substrate.[28] The electrocatalytic activity is restored in the negative-going sweep once the potential reaches the value at which PdO is reduced to Pd.

At a fixed potential of 0.7 V, current densities of 0.47 and 0.33 mA $μg_{(Pd)}^{-1}$ for Pd-(Ni-Zn)/C and Pd/C, were measured (see Figure 3). The difference of 40% in power density may explain the power output supplied by the two electroctalysts in both passive and active DGFCs investigated (vide infra). Previous studies of ethanol oxidation on Pd-(Ni-Zn)/C[25] have unambiguously shown that the Ni-based supports without Pd, though able to oxidize ethanol in alkaline media, are not directly involved in the ethanol oxidation reaction occurring at the largely negative potentials of the Pd-containing electrocatalysts. It has been proposed that Ni increases the amount of OH_{ads} groups on the catalyst surface, which would favor the formation of the carboxylic acid by coupling with acylads species. Adsorbed OH^- species are required to release the carboxylic acid. Based on these considerations, a mechanism for both the electrooxidation of EG to glycolate and G to glycerate is shown in Scheme 1.

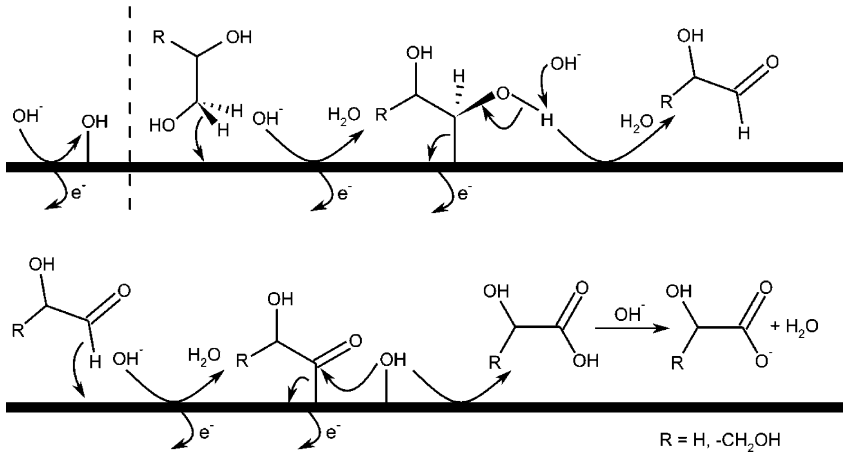

Scheme 1. Proposed mechanism for the electrooxidation of EG to glycolate and G to glycerate on Pd in alkaline media.

Passive oxygen-breathing DAFCs fuelled with EG or G containing Pd-(Ni-Zn)/C or Pd/C-catalyzed anodes

The MEAs used for the passive monoplanar DEGFCs were realized (as described in the Experimental Section) with the anode reaction catalyzed by Pd-(Ni-Zn)/C or Pd/C, Fe-Co/C as cathode, and a Tokuyama A-201 anion exchange-membrane.

The potentiodynamic and power density curves obtained with 5 wt% EG in a 2 M KOH solution at room temperature (20–22 °C) are reported in Figure 4. In the curves it is demonstrated that the cell with the Pd-(Ni-Zn)/C electrocatalyst exhibits a considerably higher open circuit voltage (OCV) and peak power density (24 mW cm^{-2} at 0.17 V) compared to the cell containing the Pd/C electrocatalyst as anode (12 mW cm^{-2} at 0.13 V). Values comparable or slightly higher (19, 22, and 28 mW cm^{-2}) have been reported by Countanceau et al., with DEGFCs (2 M EG in a 4 mol cm^{-3} NaOH), containing Pt, PtBi, and PtPdBi anode catalysts, respectively (overall metal loading

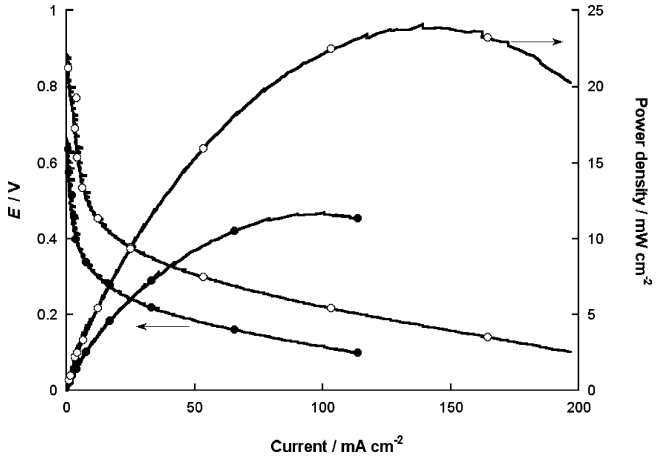

Figure 4. Potentiodynamic and power density curves at 25 °C for passive DEGFCs containing the Pd-(Ni-Zn)/C (○) and Pd/C (●) anode electrocatalysts and fuelled with 2 M KOH and 5 wt% EG solutions. The cathode was exposed to an oxygen atmosphere. Scan rate: 5 mV s^{-1}.

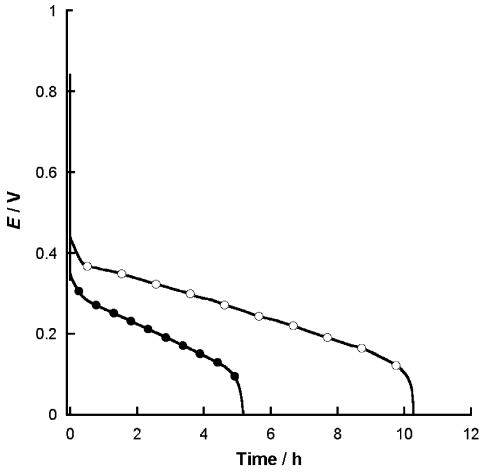

Figure 5. Galvanostatic curves (at 20 mA cm^{-2}) for the passive DEGFC containing the Pd-(Ni-Zn)/C (○) and Pd/C (●) as anode electrocatalysts and fuelled with 2 M KOH and 5 wt% EG solutions.

2 mg cm^{-2}).[21] The power output for the cell with Pd-(Ni-Zn)/C is higher than that with Pd/C in the whole potential range. This indicates that the use of the (Ni-Zn)/C-containing electrocatalyst leads to a significant increase in the fuel-cell efficiency. This is confirmed by the energy released during the galvanostatic curves (see Figure 5). Galvanostatic experiments have been performed at room temperature on the passive cells in which the anode compartment was filled with 8.47 mmol of EG. After a conditioning time of 1 h at the OCV, the circuit of the DEGFC was closed and a constant current of 20 mA cm^{-2} was allowed to flow until the cell voltage reached zero. The solution of fuel was not refueled during the experiment.

The energy released during the galvanostatic experiments was 963 J for the cell with Pd-(Ni-Zn)/C and 381 J for the cell with Pd/C. Accurate analytical quantitative and qualitative analysis of exhausts were performed by means of $^{13}C\{^1H\}$ NMR spectroscopy and ionic chromatography, using reference materials and calibration curves.

The DEGFC containing the Pd-(Ni-Zn)/C anode continued to deliver constantly 20 mA cm^{-2} for 10.2 h, yielding glycolate (55.4%), oxalate (37.6%), and carbonate (7.0%) with a total conversion of 77.1% (Figure 6, Table 3). In contrast, the DEGFC containing the Pd/C anode continued to deliver constantly 102 mA for 5.1 h, yielding glycolate (89.5%), oxalate (6.6%), and carbonate (3.6%), with a total conversion of 55.5% (Table 3). Notably, no trace of either glyoxaldehyde or hemicetal was detected at any stage of the galvanostatic experiments.

The difference in product distribution provided by Pd-(Ni-Zn)/C and Pd/C seems to be inconsistent with a similar reaction mechanism. In our previous paper investigating the electrooxidation of EG either on

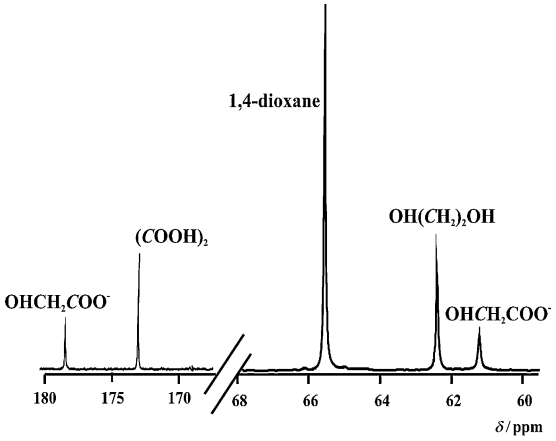

Figure 6. $^{13}C\{^1H\}$ NMR spectra at room temperature of the anode solution of a DEGFC with Pd-(Ni-Zn)/C after 10.2 h of a galvanostatic experiment at 20 mA cm^{-2}.

Pd-(Ni-Zn)/C or Pd/C, independent CV experiments were performed using solutions of potassium glycolate, potassium glyoxylate, and potassium oxalate as anolytes in an alkaline media.[23]

It was observed that the glycolate ion is much more difficult to oxidize on Pd than EG. Slightly higher current densities

Table 3. Product distribution of exhausts after galvanostatic experiments, total conversion, and released energy.

Catalyst	Product selectivity [%]							Total conversion [%]	Released energy [J]
	glycolate	oxalate	carbonate	glycerate	tartronate	oxalate	formate		
5 wt% EG; 2 M KOH									
Pd/C	89.5	6.6	3.6	–	–	–	–	55.5	381
Pd-(Ni-Zn)/C	55.4	37.6	7	–	–	–	–	77.1	963
5 wt% G; 2 M KOH									
Pd/C	11.8	13.6	28.8	15	28.4	13.6	2.4	42	366
Pd-(Ni-Zn)/C	4.2	14.1	24	27.2	28.1	14.1	2.4	55.5	578

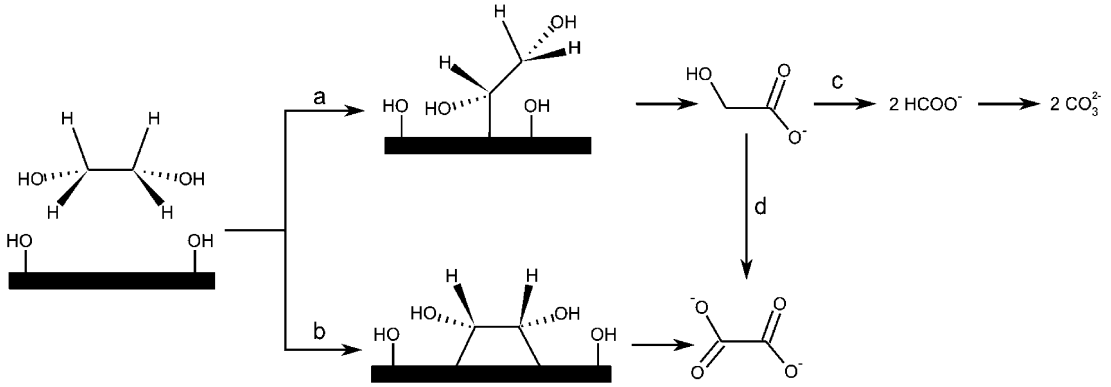

Scheme 2. Direct and sequential routes for the electrooxidation of EG.

were produced by glyoxylate, which can be an intermediate along the conversion of EG and glycolate to oxalate, whereas the oxalate was not oxidized to carbonate. Based on these considerations, as well as on the distribution of the products observed after the galvanostatic curves, a mechanism for electrooxidation of EG is proposed in Scheme 2.

Pd/C is a selective electrocatalyst, yielding 89.5% of glycolate, following preferably path a in Scheme 2. A mixture of glycolate (>50%), oxalate (37.6%), and carbonate (7.0%) are obtained with Pd-(Ni-Zn)/C (see Table 3). Carbonate is produced by oxidation of glycolate (route c), whereas the major part of oxalate seems to be produced by the direct oxidation of EG (path b). It is reasonable to assume that the Ni–Zn phase supporting the Pd nanoparticles, by virtue of nature of both Ni and Zn, might favor the chelating adsorption of EG (path b), leading preferably to the direct oxidation to oxalate.[23,31]

Polarization and power density curves obtained on passive DGFCs, containing Pd-(Ni-Zn)/C or Pd/C anodes, Fe-Co/C cathodes, and Tokuyama A-201 anion exchange-membranes, fuelled with 5 wt% G in a 2 M KOH solution and at room temperature are reported in Figure 7. In this case, under comparable conditions, the DGFC containing the Pd-(Ni-Zn)/C exhibits a higher peak power density (16.5 mW cm^{-2}) than the cell with the Pd/C electrocatalyst (8.6 mW cm^{-2}). To the best knowledge of the authors this is the most efficient electrocatalyst reported so far for the oxidation of G at room temperature. For a galvanostatic experiment performed at 20 mA cm^{-2}, without refueling, the cell potential for Pd-(Ni-Zn)/C is higher than Pd/C (Figure 8). Over 6.5 h, the energy released was 578 J for the cell with the Pd-(Ni-Zn)/C. The following product distribution was determined by NMR and ionic chromatography (IC) analysis: glycerate (27.2%), tartronate (28.1%), glycolate (4.2%), oxalate (14.1%), formate (2.4%), and carbonate (24.0%), with a total conversion of 55.5% (Figure 9, Table 3). In contrast, the DGFC equipped with Pd/C provided a current for 5.16 h, releasing 366 J of energy. About 42% of G was consumed to yield glycerate (15%), tartronate (28.4%), glycolate (11.8%), oxalate (13.6), formate (2.4%), and carbonate (28.8%). The absence of a marked difference in selectivity of G oxidation on Pd(Ni-Zn)/C and Pd/C indicates that, contrary to EG oxidation, the reaction mechanism is not substantially different for the two catalysts studied. Most importantly, both the DEGFCs and DGFCs described above were fully regenerated (same OCV and galvanostatic curves) upon replacement of the cell exhausts with

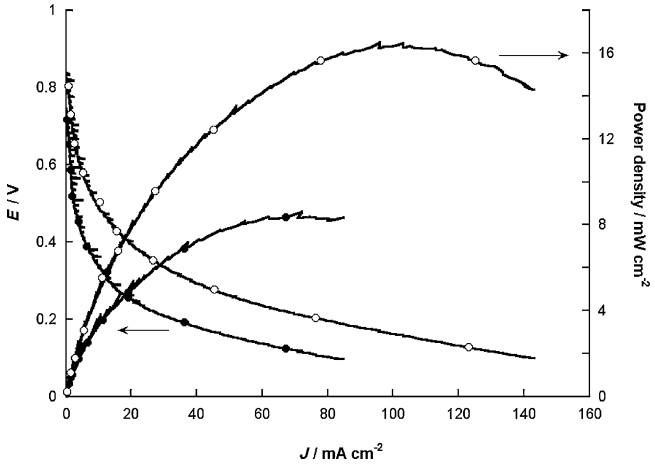

Figure 7. Potentiodynamic and power density curves at 25 °C for passive DGFCs containing the Pd-(Ni-Zn)/C (○) and Pd/C (●) anode electrocatalysts and fuelled with 2 M KOH and 5 wt% G solutions. The cathode was exposed to an oxygen atmosphere. Scan rate: 5 mV s^{-1}.

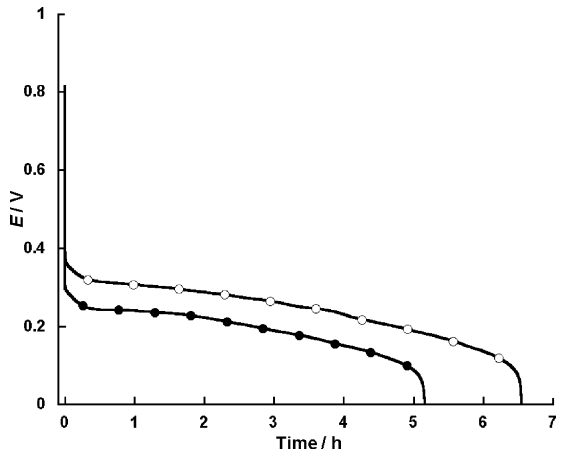

Figure 8. Galvanostatic curves (at 20 mA cm^{-2}) for the passive DGFC containing the Pd-(Ni-Zn)/C (○) and Pd/C (●) as anode electrocatalysts and fuelled with 2 M KOH and 5 wt% G solutions.

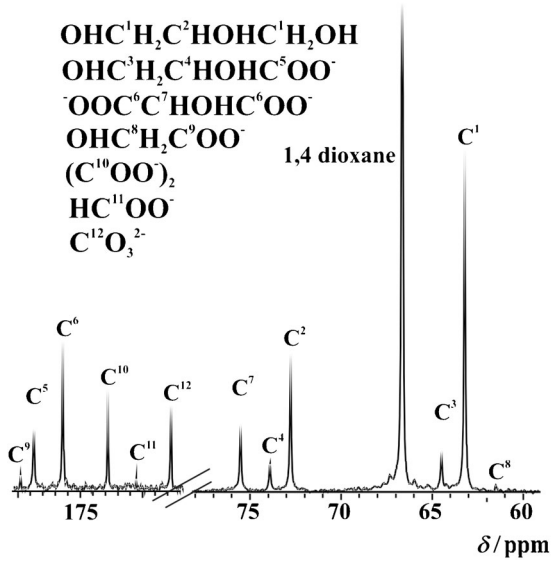

Figure 9. $^{13}C\{^1H\}$ NMR spectra at room temperature of the anode solution of a DGFC with Pd-(Ni-Zn)/C after 6.5 h of a galvanostatic experiment at 20 mA cm^{-2}.

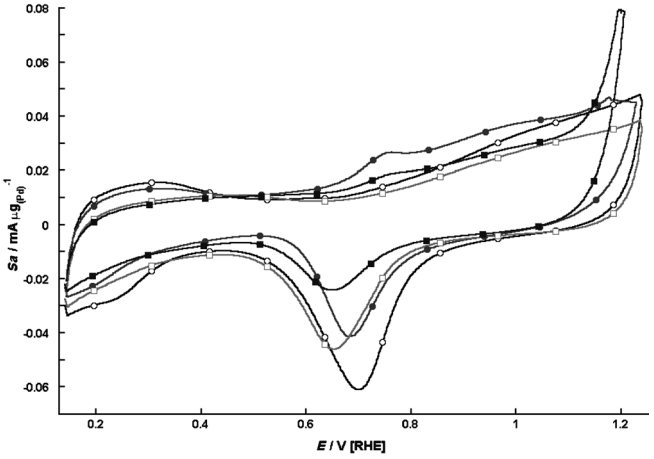

Figure 10. Cyclic voltammograms of Pd-(Ni-Zn)/C (■) and Pd/C (●) in 2 M KOH (empty symbols) or in 2 M KOH + 2 wt% tartronic acid (filled symbols). Scan rate: 50 mV s^{-1}.

a fresh 2 M KOH solution containing 5 wt% EG or G. This procedure was repeated four times with no apparent performance decay.

The oxidation of G is more complex than that of EG, in accord with the presence of three hydroxyl groups. Scheme 3 illustrates the reaction mechanism proposed for the G oxidation on both Pd-(Ni-Zn)/C and Pd/C anode catalysts. In the pathway of primary alcohol oxidation (path a), G is first oxidized to glyceraldehyde, which in turn is quickly oxidized to glycerate in a subsequent two-electron transfer step. Glycerate is further oxidized to tartronate (path a_2) and, by cleavage of C–C bond, into glycolate and formate (path a_2 and b_1). The latter species leads to carbonate and glycolate is oxidized to oxalate (path a_4).[23,24,32–34] G is also oxidized directly to tartronate (path b) by chelating adsorption on catalytic surfaces. However, the oxidation of G yields significant amounts of carbonate. Since oxalate is very slowly oxidized on Pd-based electrodes,[23,24,35–37] CO_2 is prevalently a by-product of the oxidation of either glycerate or glycolate (path a_1 and a_3). In an attempt to understand whether tartronate is oxidized to formate and glycolate (path b_1) on Pd-(Ni-Zn)/C and Pd/C, a CV study has been performed on an alkaline solution of tartronate.

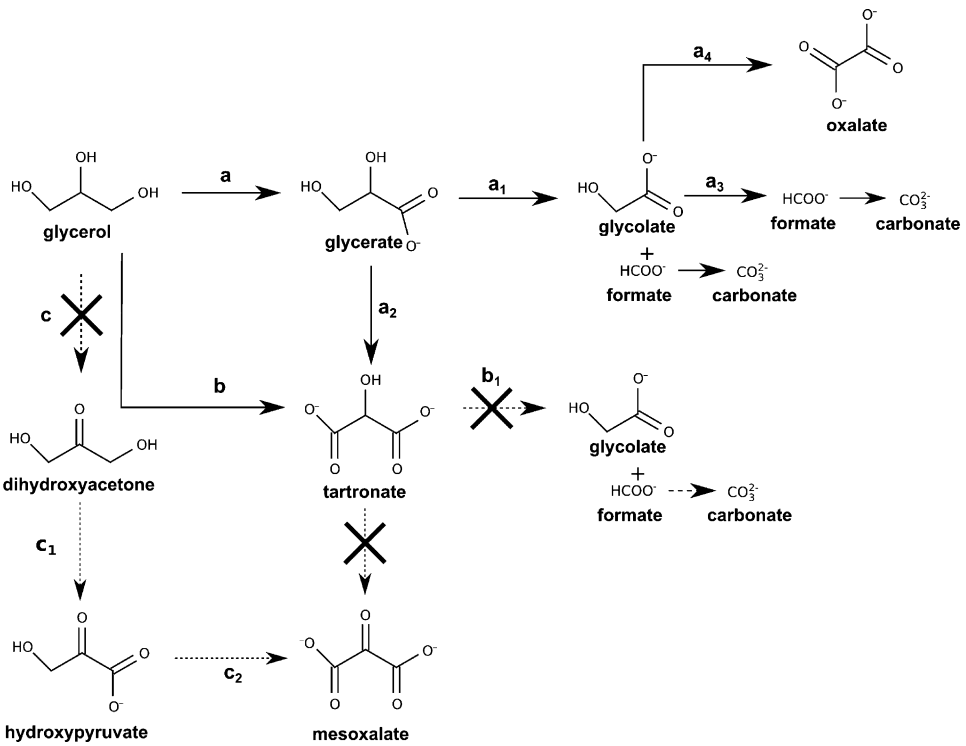

Scheme 3. Electrooxidation of G on Pd-(Ni-Zn)/C and Pd/C anode catalysts.

The corresponding cyclic voltammograms are given in Figure 10, which also shows those recorded in a KOH solution with no substrate. Upon addition of tartronic acid to the latter solutions, a significant decrease in the peak associated with PdO reduction in the reverse scan at 0.65–0.7 V is observed together with an oxidation wave at approximately 0.76 V attributable to the formation of PdO; the low specific current excludes any detectable oxidation of tartronate. Notably, no trace of dihydroxyacetone, hydroxypiruvate, or mesoxalate was detected at any stage of the galvanostatic experiments.

This evidence allows us to rule out the secondary alcohols oxidation (path c).

The oxidation of the secondary alcohols of G was reported by Koper et al.[33] on a Pt electrode, but it was not observed on an Au electrode. However, Li et al.[11,38,39] have demonstrated that this can occur both in DGFCs containing nanostructured anodic catalysts such as Pt/C (7% mesoxalic acid at 0.3 V, 2.0 M KOH + 0.1 M glycerol) and Au/C (17% glyceric acid, 39% tartronic acid, 19% mesoxalic acid, 19% and oxalic acid at 0.3 V) in which both the product selectivity and Faradaic efficiency depends on the working voltages of the fuel cell. Moreover, according to in situ infrared data obtained by Coutanceau et al.,[4] dihydroxyacetone is detected on all monometallic carbon supported catalysts (Pt/C, Pd/C, and Au/C), although hydroxypyruvate was only detected on a Au catalyst. It was proposed that an isomerization reaction of adsorbed dihydroxyacetone into adsorbed glyceraldehyde could occur with higher kinetics on Pt and Pd surfaces than on Au. Using in situ infrared spectroscopy the same absorption bands (i.e., the same oxidation species) on Pd/C as on Pt/C were observed, and it was concluded that the same mechanism was involved on both catalysts. In both cases a band located at 1335 cm^{-1} and assigned to the presence of a dihydroxyacetone species on the electrode seems to indicate that the carbon that bears the secondary alcohol group can also be oxidized at the Pt and Pd surface. Coutanceau reported that the oxidation reaction of glycerol on a $Pd_{0.5}Ni_{0.5}$/C (material not in an alloy structure), is similar to that proposed on a Pd/C catalyst, but occurring at faster kinetics. In contrast, several researchers have observed that the presence of Ni as a co-catalyst enhances the electrooxidation of alcohols in acidic or alkaline media.[25,34,40–44]

In all of our experiments no trace of the secondary alcohol oxidation of G, such as dihydroxyacetone, or products of its further oxidation, such as hydroxypyruvate or mesoxalate, were observed. This result may seem unusual, but is consistent with the fact that catalysts based on the same metal may have different particle sizes, as well as shapes or crystallinity, which could lead to different catalytic behavior owing to changes in activity as well as in selectivity.

Active DEGFCs and DGFCs

The MEAs used for the active monoplanar DEGFCs and DGFCs were realized (as described in the Experimental Section) with the anode reaction catalyzed by Pd/(Ni-Zn)/C or Pd/C (1 $mg_{(Pd)}\,cm^{-2}$), a Fe-Co/C cathode, and a Tokuyama A-201 membrane. The fuel (water solutions containing 2 M KOH and 5 wt% EG or G) was delivered to the anode (4 $mL\,min^{-1}$) and the oxygen flow was regulated (200 $mL\,min^{-1}$). Each cell temperature was regulated at 25, 40, 60, or 80 °C. For simplification, only the measurements performed at 80 °C are reported.

Figure 11 compares the potentiodynamic and power density curves at 80 °C obtained with DEGFCs realized with the anodes catalyzed by Pd-(Ni-Zn)/C and Pd/C. The cell containing the Pd-(Ni-Zn)/C electrocatalyst exhibits a higher OCV (0.9 V) and peak power density (95 $mW\,cm^{-2}$ at 0.23 V) than the cell containing the Pd/C electrocatalyst as anode (65 $mW\,cm^{-2}$ at 0.19 V).

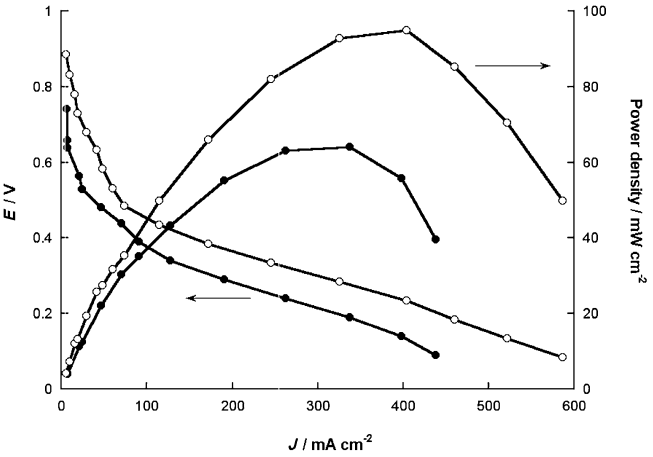

Figure 11. Potentiodynamic (scan rate 5 $mV\,s^{-1}$) and power density curves for active DEGFCs containing the Pd-(Ni-Zn)/C (○) and Pd/C (●) anode electrocatalysts fuelled with a 2 M KOH and 5 wt% EG at 80 °C.

The performance obtained with DGFCs using Pd-(Ni-Zn)/C and Pd/C anodes and fuelled with a 2 M KOH and 5 wt% G at 80 °C is reported in Figure 12. As previously observed for DEGFCs, the cell containing the Pd-(Ni-Zn)/C anode exhibits a higher peak power density (119 $mW\,cm^{-2}$ at 0.25 V) than the cell with the Pd/C electrocatalyst as anode (77 $mW\,cm^{-2}$ at 0.17 V). Notably, at 80 °C the power output of the cell with Pd-(Ni-Zn)/C increased nearly seven times, from 16.5 $mW\,cm^{-2}$ at 20 °C to 119 $mW\,cm^{-2}$ at 80 °C. Accordingly, Pd-(Ni-Zn)/C can be classified as the best-performing Pd-based electrocatalyst and amongst the best-performing electrocatalysts for EG and G oxidation.

The higher power density value provided by Pd-(Ni-Zn) indicates kinetics faster than that on Pd/C. Because of the non-alloyed structure of this electrocatalyst[25] only a bifunctional mechanism between the Ni–Zn surface providing OH^- and absorbed organic species from EG and G onto Pd nanoparticles

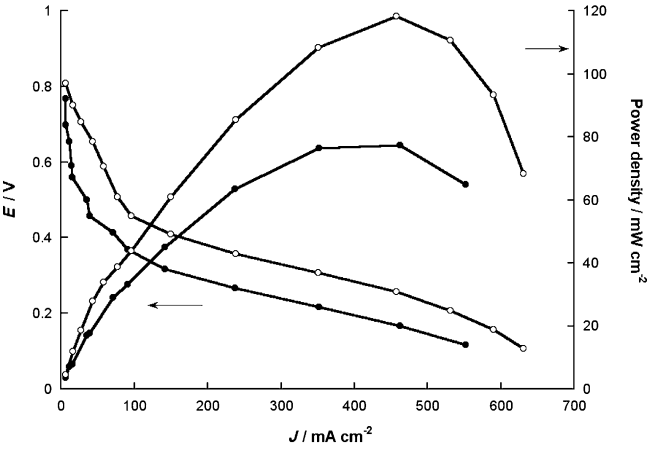

Figure 12. Potentiodynamic (scan rate 5 $mV\,s^{-1}$) and power density curves for active DGFCs containing the Pd-(Ni-Zn)/C (○) and Pd/C (●) anode electrocatalysts fuelled with a solution of 2 M KOH and 5 wt% G at 80 °C.

can be proposed to explain the catalytic improvement. A key role should be played by the capacity of Ni and NiO to generate surface Ni–OH moieties at low potentials. Increasing the amount of OH_{ads} on the catalyst surface would favor the formation of carboxylate species by coupling with Pd–$acyl_{ads}$ species, as shown in Scheme 1. In turn, the greater oxophilicity of Ni than Pd and the higher binding affinity of Ni towards the carboxylates ion may facilitate product desorption from the active Pd sites, thus accounting for the high catalytic activity of Pd-(Ni-Zn)/C.[25,42,45]

Conclusions

In this paper, examples of passive and active direct ethylene glycol fuel cells and direct glycerol fuel cells containing Pd-(Ni-Zn)/C as anode electrocatalysts (Pd nanoparticles supported on a Ni–Zn phase) are reported. A comparison with an anode electrocatalyst containing Pd nanoparticles (Pd/C) has also been presented. The oxidation of ethylene glycol (EG) and glycol (G) has primarily been investigated in half cells. The results obtained have highlighted the excellent electrocatalytic activity of Pd-(Ni-Zn)/C in terms of peak current densities (as high as 3300 $A\,g_{(Pd)}^{-1}$ for EG and 2150 $A\,g_{(Pd)}^{-1}$ for G).

Membrane-electrode assemblies (MEA) containing an anode Pd-(Ni-Zn)/C, a Fe-Co/C cathode, and a Tokuyama A-201 anion-exchange membrane have provided excellent results in monoplanar fuel cells. The MEA performance has been evaluated in passive and active cells fed with aqueous solutions of 5 wt% EG or G. Based on the peak power densities obtained in the temperature range from 20 to 80 °C and at Pd loadings at the anode as low as 1 $mg\,cm^{-2}$, to the authors' best knowledge Pd-(Ni-Zn)/C can be classified amongst the best performing electrocatalysts for EG and G oxidation.

IC and $^{13}C\{^1H\}$ NMR spectroscopy have been employed to analyze the anode exhausts of galvanostatic experiments. Pd/C is a less active but more selective electrocatalyst than Pd-(Ni-Zn)/C towards the EG oxidation, yielding 89.5% of glycolate. A mixture of glycolate (>50%), oxalate (37.6%), and carbonate (7%) was obtained with Pd-(Ni-Zn)/C. A much wider product distribution, including glycolate, glycerate, tartronate, oxalate, formate, and carbonate, was detected from the oxidation of glycerol with both Pd/C and Pd-(Ni-Zn)/C. No trace of the secondary alcohol oxidation products of G such as dihydroxyacetone, hydroxypiruvate, or mesoxalate was observed.

The remarkable electrocatalytic activity of Pd-(Ni-Zn) can be associated both with the high dispersion of the metal particles and to the intrinsic properties of the Ni–Zn phase that should increase the amount of OH_{ads} groups on the catalyst surface, which are required for the formation of carboxylic acids.

Experimental Section

Materials and general instrumentation.

All manipulations, except as stated otherwise, were routinely performed under a nitrogen atmosphere using standard airless technique. Carbon black (Vulcan XC-72 pellets) was purchased from Cabot Corp., USA. The Fe-Co/C cathode electrocatalyst [C = Ketjen Black; inductively coupled plasma (ICP) analysis: 1.13 wt% Fe and 1.71 wt% Co] was prepared by a method reported elsewhere.[26] The alkaline solid electrolyte used in both passive and active DAFCs was a anion-exchange membrane A-201 (OH^- type) obtained from Tokuyama Corporation. All metal salts and reagents were purchased from Aldrich and used as received. All the solutions were freshly prepared with doubly distilled deionized water. The quantitative analysis of the FC cell exhausts was obtained by $^{13}C\{^1H\}$-NMR spectroscopy (Bruker Avance DRX-400) with chemical shifts relative to external tetramethylsilane. The calibration curves for the quantitative analysis were obtained using authentic samples of the various products in the appropriate range of concentrations and using 1,4-dioxane as internal standard. IC was also used to identify the oxidation products (Metrohm 761 Compact equipped with a Metrosep Organic Acids column). The sonication process was performed with a Bandelin Sonopuls probe instrument.

Synthesis of electrocatalysts

The electrocatalysts Pd-(Ni-Zn)/C and Pd/C were prepared as previously described.[25]

Pd/C: Vulcan XC-72 (5.94 g) was sonicated (20 min) in a three-necked round-bottomed flask (500 mL) containing ethylene glycol (250 mL). An aqueous solution (50 mL) obtained by treatment of $PdCl_2$ (0.6 g, 3.38 mmol) with 6 mL of HCl (37% *w/w*) was added dropwise to the resulting dispersion with stirring. After addition of the Pd salt, a solution of NaOH (5.1 g) in water (10 mL) was introduced into the reactor, which was then heated (to 140 °C) under a nitrogen atmosphere (3 h). Afterwards, the reaction mixture was allowed to cool to room temperature and the solid product was filtered off under nitrogen atmosphere and washed with distilled water to neutral pH. The final product was dried (40 °C, under vacuum) to constant weight. The yield was 5.8 g. Inductively coupled plasma atomic emission spectroscopy (ICP-AES) analysis revealed a Pd content of 5.2 wt%.

Pd-(Ni-Zn)/C: A slurry of Zn powder (2.8 g, 43 mmol) and Vulcan XC-72 (6.0 g) in H_2O (40 mL) in a three-necked round-bottomed flask (100 mL) was sonicated (20 min). The slurry was heated (90 °C), and then a solution of NiCl2·6 H2O (5.06 g, 21.28 mmol) in water (10 mL) was added under vigorous stirring (within 1–2 min). Foaming was observed owing to gas evolution that gradually disappeared (3–4 min). The resulting reaction mixture was stirred at (RT, 30 min), then the solid product was filtered off and washed portion-wise with hot water (50 °C; 200 mL). This solid was suspended in an aqueous solution of NaOH (13 wt%; 300 mL), and the suspension was stirred until no H_2 gas evolution was evident (40 min). The final product was separated from the reaction mixture by filtration and washed with distilled H_2O to neutral pH. A small portion of this product was dried with a stream of nitrogen and analyzed by ICP-AES (wt%; Ni 14.4, Zn 3.4). The solid product was suspended in water (400 mL), and the resulting slurry was sonicated (30 min). A solution of K_2PdCl_4 (1 g, 3.01 mmol) in water (250 mL) was slowly added (ca. 3 h) to this suspension under vigorous stirring, and the reaction mixture was gently stirred overnight at room temperature. The final product was filtered off, washed with water (4×100 mL), and dried (40 °C under vacuum) to constant weight. Yield: 6.0 g. ICP-AES (wt%): Pd 6.4, Ni 9.7, Zn 2.6.

Half-cell testing

A portion (about 45 mg) of each electrocatalyst was introduced into a high-density polyethylene container (5 mL) together with water (1.2 g), ethanol (99.8%, 0.70 g, Fluka) and a Tokuyama OH^--type anion-exchange ionomer in alcohols solution (0.19 g). The resulting suspension was sonicated (90 min) using a FALC ultrasonic bath. Each suspension was freshly prepared just before carrying out the experiment scheduled. The metal loading on each electrode was determined by weighting the amount of the deposited ink onto the glassy carbon electrode. Cyclic voltammetry (CV) experiments were conducted on a Parstat 2273A potentiostat/galvanostat (Princeton Applied Research), using a three-electrode arrangement with a saturated $Ag/AgCl/KCl_{sat}$ reference electrode and a platinum wire as counter electrode. The potential scale of the CV curves was expressed according to the RHE.

Fuel-Cell Testing

Passive breathing fuel cells. The MEAs (membrane electrode assembly) for the passive monoplanar cells were realized using a commercial Tokuyama A-201 anion-exchange membrane and cathodes containing a proprietary Fe-Co/C electrocatalyst.[26] The cell hardware was described previously.[24] The membrane was conditioned in a saturated KOH solution (1 h) before assembling the MEA. The anode was realized with a nickel foam plate (5.13 cm^2) onto which the appropriate amount of dense catalytic ink was deposited. This was prepared by introducing the catalyst (about 100 mg) into a polyethylene container (5 mL) together with water (about 80 mg). The metal loading on each electrode ($\approx$ 1 mg cm^{-2}), was determined by weighing the amount of ink deposited. The MEA was obtained by mechanically pressing the anode, cathode, and membrane at approximately 40 bar. For a reliable evaluation of the oxidation products, the anode compartment was sealed under a nitrogen atmosphere while the cathode was exposed to either air or oxygen with no significant variation in the cell performance. This was evaluated by means of an ARBIN BT-2000 5A 4 channels instrument. The fuel oxidation products were qualitatively and quantitatively determined by IC and $^{13}C\{^1H\}$-NMR spectroscopy using appropriate calibration curves.

Active breathing fuel cells. The active fuel cell system, purchased from Scribner-Associates (USA) with a 25 cm^2 fuel cell fixture and an effective electrode area of 5 cm^2, was modified in our laboratory with titanium end plates to tolerate the alkaline conditions. The MEA was fabricated by mechanically pressing at approximately 100 bar the anode (nickel foam), cathode (carbon cloth) and Tokuyama A-201 alkaline exchange membrane. A dense anode ink was prepared by mixing the powdered catalyst with an aqueous dispersion of polytetrafluoroethylene (PTFE) to produce a binder loading of 5 wt%. As a general procedure, an identical amount of the resulting paste was spread onto two identical Ni-foam plates. One of these was used almost immediately to fabricate the MEA, the other was dried until constant weight for the quantitative determination of the Pd loading ($\approx$1 mg cm^{-2} in all cases). The fuel (water solution containing 5 wt% EG or G in 2 M KOH) was delivered to the anode (4 mL min^{-1}) and regulated at 25, 40, 60, and 80 °C, respectively. The oxygen flow (200 mL min^{-1})was regulated at 25, 30, 40, and 60 °C, respectively (RH 100%). The temperature of the cell under working conditions was controlled at 25, 40, 60, and 80 °C, respectively, by a thermocouple positioned inside the end plate at the cathode side.

Acknowledgements

The authors acknowledge the financial support from: Ing. Guido Gay (Switzerland) project: "Conversion of CO_2 in hydrocarbons and oxygenated compounds"; the MATTM (Italy) for the PIRODE project no 94; the MSE for the PRIT project Industria 2015; the MIUR (Italy) for the FIRB 2010 project RBFR10J4H7_002.

Keywords: electrochemistry · fuel cells · nanoparticles · oxidation · palladium

[1] F. Alcaide, P. L. Cabot, E. Brillas, *J. Power Sources* **2006**, *153*, 47 – 60.
[2] N. Ji, T. Zhang, M. Y. Zheng, A. Q. Wang, H. Wang, X. D. Wang, J. G. G. Chen, *Angew. Chem.* **2008**, *120*, 8638 – 8641; *Angew. Chem. Int. Ed.* **2008**, *47*, 8510 – 8513.
[3] M. Y. Zheng, A. Q. Wang, N. Ji, J. F. Pang, X. D. Wang, T. Zhang, *ChemSusChem* **2010**, *3*, 63 – 66.
[4] M. Simões, S. Baranton, C. Coutanceau, *Appl. Catal. B* **2010**, *93*, 354 – 362.
[5] A. Behr, J. Eilting, K. Irawadi, J. Leschinski, F. Lindner, *Green Chem.* **2008**, *10*, 13 – 30.
[6] S. Carrettin, P. McMorn, P. Johnston, K. Griffin, C. J. Kiely, G. J. Hutchings, *Phys. Chem. Chem. Phys.* **2003**, *5*, 1329 – 1336.
[7] L. Prati, P. Spontoni, A. Gaiassi, *Top. Catal.* **2009**, *52*, 288 – 296.
[8] D. Liang, J. Gao, J. H. Wang, P. Chen, Z. Y. Hou, X. M. Zheng, *Catal. Commun.* **2009**, *10*, 1586 – 1590.
[9] A. Villa, G. M. Veith, L. Prati, *Angew. Chem.* **2010**, *122*, 4601 – 4604; *Angew. Chem. Int. Ed.* **2010**, *49*, 4499 – 4502.
[10] S. Carrettin, P. McMorn, P. Johnston, K. Griffin, G. J. Hutchings, *Chem. Commun.* **2002**, 696 – 697.
[11] L. Xin, Z. Zhang, J. Qi, D. Chadderdon, W. Li, *Appl. Catal. B* **2012**, *125*, 85 – 94.
[12] Z. Zhang, L. Xin, W. Li, *Appl. Catal. B* **2012**, *119 – 120*, 40 – 48.
[13] A. Ilie, M. Simões, S. Baranton, C. Coutanceau, S. Martemianov, *J. Power Sources* **2011**, *196*, 4965 – 4971.
[14] A. Falase, M. Main, K. Garcia, A. Serov, C. Lau, P. Atanossov, *Electrochim. Acta* **2012**, *66*, 295 – 301.
[15] Y. Kwon, Y. Birdja, I. Spanos, P. Rodriguez, M. T. Koper, *ACS Catal.* **2012**, *2*, 759 – 764.
[16] P. K. Shen, C. Xu, *Electrochem. Commun.* **2006**, *8*, 184 – 188.
[17] Z. Wang, F. Hu, P. K. Shen, *Electrochem. Commun.* **2006**, *8*, 1764 – 1768.
[18] C. W. Xu, P. K. Shen, Y. J. Liu, *J. Power Sources* **2007**, *164*, 527 – 553.
[19] F. P. Hu, G. F. Cui, Z. D. Wei, P. K. Shen, *Electrochem. Commun.* **2008**, *10*, 1303 – 1306.
[20] C. Coutanceau, L. Demarconnay, C. Lamy, J. M. Léger, *J. Power Sources* **2006**, *156*, 14 – 19.
[21] L. Demarconnay, S. Brimaud, C. Coutanceau, J. M. Léger, *J. Electroanal. Chem.* **2007**, *601*, 169 – 180.
[22] M. Simões, S. Baranton, C. Coutanceau, *Appl. Catal. B* **2011**, *110*, 40 – 49.
[23] V. Bambagioni, M. Bevilacqua, C. Bianchini, J. Filippi, A. Marchionni, F. Vizza, L. Q. Wang, P. K. Shen, *Fuel Cells* **2010**, *10*, 582 – 590.
[24] V. Bambagioni, C. Bianchini, A. Marchionni, J. Filippi, F. Vizza, J. Teddy, P. Serp, M. Zhiani, *J. Power Sources* **2009**, *190*, 241 – 251.
[25] V. Bambagioni, C. Bianchini, J. Filippi, W. Oberhauser, A. Marchionni, F. Vizza, R. Psaro, L. Sordelli, M. L. Foresti, M. Innocenti, *ChemSusChem* **2009**, *2*, 99 – 112.
[26] V. Bambagioni, C. Bianchini, J. Filippi, A. Lavacchi, W. Oberhauser, A. Marchionni, S. Moneti, F. Vizza, R. Psaro, V. Dal Santo, A. Gallo, S. Recchia, L. Sordelli, *J. Power Sources* **2011**, *196*, 2519 – 2529.
[27] E. Santos, M. C. Giordano, *Electrochim. Acta* **1985**, *30*, 871 – 878.
[28] Z. X. Liang, T. S. Zhao, J. B. Xu, L. D. Zhu, *Electrochim. Acta* **2009**, *54*, 2203 – 2208.
[29] N. Dalbay, F. Kadirgan, *J. Electroanal. Chem.* **1990**, *296*, 559 – 569.
[30] C. Xu, Z. Tian, P. K. Shen, S. P. Jiang, *Electrochim. Acta* **2008**, *53*, 2610 – 2618.
[31] L. Roquet, E. M. Belgsir, J.-M. Léger, C. Lamy, *Electrochim. Acta* **1994**, *39*, 2387 – 2394.

[32] J.-L. Lin, J. Ren, N. Tian, Z.-Y. Zhan, S.-G. Sun, *J. Electroanal. Chem.* DOI: 10.1016/j.jelechem.2012.08.027.
[33] Y. Kwon, K. J. P. Schouten, M. T. M. Koper, *ChemCatChem* **2011**, *3*, 1176 – 1185.
[34] C. Bianchini, P. K. Shen, *Chem. Rev.* **2009**, *109*, 4183 – 4206.
[35] H. T. Zheng, Y. Li, S. Chen, P. K. Shen, *J. Power Sources* **2006**, *163*, 371 – 375.
[36] P. Bert, C. Bianchini, G. Giambastiani, A. Marchionni, A. Tampucci, F. Vizza, PCT/EP 2008/055706.
[37] a) F. Hahn, B. Beden, F. Kadirgan, C. J. Lamy, *J. Electroanal. Chem.* **1987**, *216*, 169 – 180; b) P. A. Christensen, A. Hamnett, *J. Electroanal. Chem.* **1989**, *260*, 347 – 359.
[38] L. Xin, Z. Zhang, Z. Wang, W. Li, *ChemCatChem* **2012**, *4*, 1105 – 1114.
[39] Z. Zhang, L. Xin, W. Li, *Int. J. Hydrogen Energy* **2012**, *37*, 9393 – 9401.
[40] K. S. Kumar, P. Haridoss, S. K. Seshadri, *Surf. Coat. Technol.* **2008**, *202*, 1764 – 1770.
[41] R. N. Singh, A. Singh, Anindita, *Int. J. Hydrogen Energy* **2009**, *34*, 2052 – 2057.
[42] C. Bianchini, V. Bambagioni, J. Filippi, A. Marchionni, F. Vizza, P. Bert, A. Tampucci, *Electrochem. Commun.* **2009**, *11*, 1077 – 1080.
[43] M. R. Tarasevich, Z. R. Karichev, V. A. Bogdanovskaya, E. N. Lubnin, A. V. Kapustin, *Electrochem. Commun.* **2005**, *7*, 141 – 146.
[44] S. Sen Gupta, J. Datta, *J. Power Sources* **2005**, *145*, 124 – 132.
[45] V. Bambagioni, C. Bianchini, Y. Chen, J. Filippi, P. Fornasiero, M. Innocenti, A. Lavacchi, A. Marchionni, W. Oberhauser, F. Vizza, *ChemSusChem* **2012**, *5*, 1266 – 1273.

Received: November 12, 2012
Published online on February 12, 2013